

1 **The age-dependent relationship between resting heart rate variability**
2 **and functional brain connectivity**

3
4 D. Kumral^{1,2}, H.L. Schaare^{1,3}, F. Beyer^{1,4}, J. Reinelt¹, M. Uhlig^{1,3},

5 F. Liem¹, L. Lampe¹, A. Babayan¹, A. Reiter^{5,1}, M. Erbey², J. Roebbig¹, M. Loeffler⁶,

6 M.L. Schroeter^{1,6,7}, D. Husser⁸, A.V. Witte¹, A. Villringer^{1,2,4,6,9}, M. Gaebler^{1,2,6}

7
8 ¹ Department of Neurology, Max Planck Institute for Human Cognitive and Brain Sciences,
9 Leipzig, Germany

10 ² MindBrainBody Institute at the Berlin School of Mind and Brain, Humboldt-Universitaet
11 zu Berlin, Berlin, Germany

12 ³ International Max Planck Research School NeuroCom, Leipzig, Germany

13 ⁴ Subproject A1, Collaborative Research Centre 1052 “Obesity Mechanisms”, University of
14 Leipzig, Leipzig, Germany

15 ⁵ Lifespan Developmental Neuroscience, Technical University of Dresden, Dresden, Germany

16 ⁶ LIFE – Leipzig Research Center for Civilization Diseases, University of Leipzig, Leipzig,
17 Germany

18 ⁷ Department of Cognitive Neurology, University of Leipzig, Leipzig, Germany

19 ⁸ Department of Electrophysiology, Leipzig Heart Centre, University of Leipzig, Leipzig,
20 Germany

21 ⁹ Center for Stroke Research Berlin, Charité – Universitaetsmedizin Berlin, Berlin, Germany

22
23
24
25
26
27
28
29
30
31
32
33
34
35
36
37
38
39
40
41
42
43
44
45

Abstract

Resting heart rate variability (HRV), an index of parasympathetic cardiorespiration and an individual trait marker related to mental and physical health, decreases with age. Previous studies have associated resting HRV with structural and functional properties of the brain – mainly in cortical midline and limbic structures. We hypothesized that HRV may alter its relationship with brain structure and function across the adult lifespan. In 388 healthy subjects of three age groups (140 younger: 26.0±4.2 years, 119 middle-aged: 46.3±6.2 years, 129 older: 66.9±4.7 years), gray matter structure (voxel-based morphometry) and resting-state functional connectivity (eigenvector centrality mapping and exploratory seed-based functional connectivity) were related to resting HRV, measured as the root mean square of successive differences (RMSSD). Confirming previous findings, resting HRV decreased with age. For HRV-related gray matter volume, there were no statistically significant differences between the age groups, nor similarities across all age groups. In whole-brain functional connectivity analyses, we found an age-dependent association between resting HRV and eigenvector centrality in the bilateral ventromedial prefrontal cortex (vmPFC), driven by the younger adults. Across all age groups, HRV was positively correlated with network centrality in bilateral posterior cingulate cortex. Seed-based functional connectivity analysis using the vmPFC cluster revealed an HRV-related cortico-cerebellar network in younger but not in middle-aged or older adults. Our results indicate that the decrease of HRV with age is accompanied by changes in functional connectivity along the cortical midline. This extends our knowledge of brain-body interactions and their changes over the lifespan.

Keywords: heart rate variability, aging, eigenvector centrality mapping, brain structure, voxel-based morphometry, default mode network

46

1. Introduction

47 Behavioral and physiological changes that occur with advancing age become manifest in
48 the structure and function of multiple macro- and micro-systems of the human organism
49 (Arking, 2006). Important alterations occur in the cardiovascular and the nervous systems,
50 which are coupled to react dynamically to environmental demands (McEwen, 2003). Such
51 adaptations to internal and external challenges, while leaving an imprint on body and brain,
52 underlie healthy aging (Lipsitz and Goldberger, 1992; Swank, 1996). They are also reflected
53 in brain-heart interactions – particularly in parasympathetic cardioregulation – that can be
54 measured as resting heart rate variability (HRV)

55 HRV quantifies variations in the cardiac beat-to-beat (or RR) interval that can be
56 measured with an electrocardiogram (ECG). Phasic modulation of the heart rate arises from
57 the influences of both branches of the autonomic nervous system (ANS), the parasympathetic
58 (PNS) and the sympathetic nervous system (SNS) – with the PNS quickly lowering the heart
59 rate and the SNS slowly increasing it. Because the PNS has very short response latencies,
60 HRV – and some HRV measures more than others – represents parasympathetic (i.e., vagal)
61 influences on the heart (Thayer and Lane, 2007). HRV, typically acquired at rest, is known to
62 decrease with age (De Meersman and Stein, 2007; Umetani et al., 1998). Preservation of
63 autonomic function, as indexed by relatively increased HRV, has been shown a prerequisite
64 for longevity and healthy aging (Zulfiqar et al., 2010). Higher HRV has also been associated
65 with higher health (Kemp and Quintana, 2013) – for example, with less cardiovascular
66 diseases (Liao et al., 1997; Thayer et al., 2010) – and reduced overall mortality (Bucelletti et
67 al., 2009). In older adults, HRV can indicate inter-individual differences in cognitive
68 performance (Mahinrad et al., 2016; Zeki Al Hazzouri et al., 2014). Hence, resting HRV
69 could be regarded as a biomarker of healthy aging.

70 The neurovisceral integration model considers the role of the brain in parasympathetic
71 cardiorespiration and provides a framework to explain individual differences in resting vagal
72 function (Kemp et al., 2017; Thayer et al., 2012). According to this model, frontal and
73 midbrain areas interact and the prefrontal cortex (PFC) inhibits subcortical regions as well as
74 the ANS. Thereby, the heart is under tonic inhibitory control by the ANS. Assuming this close
75 interaction of the brain and the ANS in heart rate regulation, it has been suggested that inter-
76 individual differences in HRV may reflect structural and functional variability in the brain
77 (Thayer et al., 2012). Indeed, inter-individual differences in resting HRV have been
78 associated with cortical thickness in right anterior midcingulate cortex (amCC) (Winkelmann
79 et al., 2017) as well as in rostral anterior cingulate cortex (ACC) and left lateral orbitofrontal
80 cortex (OFC) (Yoo et al., 2017). A recent study in individuals between 20 and 60 years found
81 a negative correlation between resting HRV and gray matter volume in limbic structures like
82 insula, amygdala, and parahippocampal gyrus (Wei et al., 2018). Similar brain regions have
83 also been related to HRV in functional neuroimaging studies (Holzman and Bridgett, 2017;
84 Mather and Thayer, 2018; Thayer et al., 2012); both task-based (e.g., BOLD: Critchley et al.,
85 2000; regional cerebral blood flow; rCBF: Gianaros et al., 2004; meta-analyses: Beissner et
86 al., 2013; Thayer et al., 2012) and under resting state conditions (Chang et al., 2013; Jennings
87 et al., 2016; Sakaki et al., 2016). In these studies, activation and connectivity in the medial
88 prefrontal cortex (mPFC), anterior cingulate cortex (ACC), and posterior cingulate cortex
89 (PCC) have most consistently been associated with HRV. These brain areas involved in
90 parasympathetic cardiorespiration overlap with the default mode network (DMN) and
91 particularly its nodes along the cortical midline (Beissner et al., 2013). However, the only
92 fMRI study that investigated heart-brain interactions across the adult lifespan included 17
93 younger and 18 older subjects and restricted their analyses to *a priori* defined regions-of-
94 interest (Sakaki et al., 2016). Across all subjects, higher HRV was related to stronger

95 functional connectivity between right amygdala and medial prefrontal regions, while age
96 group differences were found in HRV-related connectivity between right amygdala and lateral
97 prefrontal regions.

98 We here investigated brain-heart interactions across the adult lifespan by combining
99 measures of brain structure and function with the assessment of resting HRV. The main aims
100 of this study were to examine (i) the relationship between resting HRV, brain structure, and
101 functional connectivity as well as (ii) its dependence on age in a large sample of healthy
102 adults across the lifespan. Based on previous findings (reviewed above), we hypothesized that
103 inter-individual differences in the brain correlate with inter-individual differences in resting
104 HRV and that this correlation changes with age. To detect HRV-related structural alterations,
105 we used voxel-based morphometry (VBM) (Ashburner and Friston, 2000). To assess HRV-
106 related changes in the functional architecture across the whole brain, we used the graph-based
107 method of eigenvector centrality mapping (ECM). ECM can identify important network nodes
108 (in this case: voxels) based on their functional connectivity (similar to Google's page rank
109 algorithm) and without the need of an *a priori* selection of a specific seed region or the
110 number of networks / components (Lohmann et al., 2010; Wink et al., 2012). To further
111 explore ECM-derived whole-brain connectivity patterns, we also implemented a resting-state
112 seed-based connectivity analysis (for more details see *Methods*).

113 2. Methods

114 2.1. Participants

115 Data from two studies were used: (I) the Leipzig Research Centre for Civilization
116 Diseases (LIFE; Loeffler et al., 2015) and (II) the “Leipzig Study for Mind-Body-Emotion
117 Interactions” (LEMON; Babayan et al., under review).

118 LIFE is a large population-based cohort study from Leipzig, Germany (Loeffler et al.,
119 2015). From the sample of LIFE subjects with MRI data ($n = 2,667$), we selected healthy
120 subjects between the ages of 20 and 80 years. We applied strict exclusion criteria in three
121 categories: I) health-related criteria; participants were excluded if they reported any
122 medication intake except vitamin food supplements, any past or present cardiovascular health
123 problems and diagnoses, or surgeries, any other medical history and/or diagnosis, in a medical
124 interview. II) ECG-related criteria (see details on ECG acquisition below); if a subject had
125 more than one ECG recording, we used the first acquired ECG file that was collected on the
126 same day as the MRI acquisition. Otherwise, we selected the ECG recording that was
127 temporally closest to MRI acquisition. Regarding data quality, we excluded data with
128 unrepairable signal artifacts or problems regarding R-peak detection. We also omitted data
129 with any abnormal ECG signal (e.g., supraventricular extrasystoles) after visual inspection as
130 well as subjects with extreme HRV values based on Tukey’s (1977) criterion of 3 interquartile
131 ranges (IQR) above the LIFE sample median ($N=14$, *Median*: 30.13, *IQR*: 29.76). III) MRI-
132 related criteria; we excluded subjects with incidental findings (e.g., brain tumor, multiple
133 sclerosis, or stroke) on T1-weighted and/or fluid-attenuated inversion recovery (FLAIR)
134 images. We further excluded subjects based on rs-fMRI quality assessment, for example with
135 faulty preprocessing (e.g., during denoising) or excessive head motion (criterion: mean
136 framewise displacement (FD) > 0.6 mm; Power et al., 2012).

137 LEMON is a cross-sectional sample of healthy younger and older subjects from
138 Leipzig, Germany, who had never participated in another “psychological or MRI research”-
139 related study, did not report any neurological disorders, head injury, any medication affecting
140 the cardiovascular and/or central nervous system, alcohol or other substance abuse,
141 hypertension, pregnancy, claustrophobia, chemotherapy and malignant diseases, current
142 and/or previous psychiatric disease (Babayan et al., under review). The LEMON sample
143 comprised 171 eligible subjects divided into two age groups (young: 20-35 years, old: 59-75
144 years). Similar to the exclusion criteria mentioned above, subjects with incomplete data (N =
145 38), incidental findings in MRI (FLAIR, T2-weighted, T1-weighted, SWI) (N=7), or
146 psychoactive drug intake (e.g., tetrahydrocannabinol) determined by urine test (N = 9) were
147 excluded. Two subjects were discarded due to the HRV outlier criterion mentioned above
148 (LEMON sample *Median*: 40.62, *IQR*: 39.82) and five subjects due to excessive head motion
149 (mean FD > 0.6 mm; Power et al., 2012). To increase the statistical power and the
150 comparability, we pooled the two samples and divided them into three age groups: young (20-
151 35 years from LIFE and LEMON), middle-aged (35-60 years from LIFE), and old (60-80
152 years from LIFE and LEMON). Details are provided in Table 1.
153 Both studies were in agreement with the Declaration of Helsinki and approved by the ethics
154 committee of the medical faculty at the University of Leipzig, Germany.

155 2.2.ECG collection and HRV analysis

156 *LIFE sample*. Ten seconds of a standard medical 12-lead resting ECG were acquired
157 using a Page-Writer TC50 ECG system (Philips Medical Systems, Amsterdam, Netherlands)
158 in supine position. We used lead I (from Einthoven’s triangle) for the analysis. R-peaks were
159 automatically detected using the findpeaks function in Matlab 9 (The MathWorks, Inc.,
160 Natick, Massachusetts) or Kubios 2.2 (Tarvainen et al., 2014). The ECG data for each subject
161 was manually checked for physiological or computational artifacts like supraventricular

162 extrasystoles or faulty peak detection, respectively. From RR interval time series (i.e.,
163 tachograms), we calculated the root mean square of successive differences (RMSSD) of
164 adjacent RR intervals (Task Force of the European Society of Cardiology and the North
165 American Society of Pacing Electrophysiology, 1996).

166 *LEMON sample.* Four minutes of resting ECG were acquired using a Biopac MP35
167 amplifier with the acquisition software AcqKnowledge version 4.0 (Biopac Systems
168 Inc., <http://www.biopac.com>, Goleta, CA, USA) and three disposable electrodes on the
169 thorax: the reference electrode was attached near the right collarbone, the measuring electrode
170 on the left-hand side of the body on the same level as the 10th rib, and the ground electrode on
171 the right hip bone. The subjects were instructed to think about daily routines, relax, and
172 breathe at a comfortable rate in sitting position. The peak detection and RMSSD calculation
173 were performed using Kubios 2.2 (Tarvainen et al., 2014).

174 RMSSD values of our sample were natural log-transformed to obtain normally
175 distributed data (Shapiro-Wilk tests; $W = 0.99$, $p = 0.12$). In the rest of the paper, log-
176 transformed RMSSD will be referred to as “HRV”.

177 2.3.MRI acquisition

178 Brain imaging for both datasets was performed on the same 3T Siemens Magnetom
179 Verio MR scanner (Siemens Medical Systems, Erlangen, Germany) with a standard 32-
180 channel head coil. In both samples, subjects were instructed to keep their eyes open and not to
181 fall asleep during the acquisition period.

182 *LIFE sample.* The structural T1-weighted images were acquired using a generalized
183 auto-calibrating partially parallel acquisition technique (Griswold et al., 2002) and the
184 Alzheimer’s Disease Neuroimaging Initiative standard protocol with the following
185 parameters: inversion time (TI) = 900 ms, repetition time (TR) = 2.3 ms, echo time (TE) =
186 2.98 ms, flip angle (FA) = 9°, band width = 240 Hz/pixel, field of view (FOV) = 256 x 240 x

187 176 mm³, voxel size = 1 x 1 x 1 mm³, no interpolation. T2*-weighted functional images were
188 acquired using an echo-planar-imaging (EPI) sequence with the following parameters: TR =
189 2000 ms, TE= 30 ms, FA = 90°, FOV = 192 x 192 x 144 mm³, voxel size = 3 mm x 3 mm,
190 slice thickness = 4 mm, slice gap = 0.8 mm, 300 volumes, duration = 10.04 min. A gradient
191 echo field map with the sample geometry was used for distortion correction (TR = 488 ms,
192 TE 1 = 5.19 ms, TE 2 = 7.65 ms).

193 *LEMON sample.* The structural image was recorded using an MP2RAGE sequence
194 (Marques et al., 2010) with the following parameters: TI 1 = 700 ms, TI 2 = 2500 ms, TR =
195 5000 ms, TE = 2.92 ms, FA 1 = 4°, FA 2 = 5°, band width = 240 Hz/pixel, FOV = 256 × 240
196 × 176 mm³, voxel size = 1 x 1 x 1 mm³. The functional images were acquired using a T2*
197 weighted multiband EPI sequence with the following parameters: TR = 1400 ms, TE = 30 ms,
198 FA= 69°, FOV = 202 mm, voxel size = 2.3 x 2.3 x 2.3 mm³, slice thickness = 2.3 mm, slice
199 gap = 0.67 mm, 657 volumes, multiband acceleration factor = 4, duration = 15.30 min. A
200 gradient echo field map with the sample geometry was used for distortion correction (TR =
201 680 ms, TE 1 = 5.19 ms, TE 2 = 7.65 ms).

202 2.4.MR data preprocessing and analysis

203 *Structural MRI.* We analyzed structural brain alterations on the T1-weighted 3D image
204 using VBM (Ashburner and Friston, 2000) as implemented in SPM12 (Wellcome Trust
205 Centre for Neuroimaging, UCL, London, UK) and the Computational Anatomy Toolbox
206 (CAT12: <http://dbm.neuro.uni-jena.de/cat/>), running on Matlab 9.3 (Mathworks, Natick, MA,
207 USA). In the LEMON sample before the preprocessing, we removed the background noise
208 from MP2RAGE on the computed uniform images via masking (Streitbürger et al., 2014).
209 The preprocessing steps consisted of segmentation, bias-correction, and normalization using
210 high-dimension Diffeomorphic Anatomical Registration Through Exponentiated Lie Algebra
211 (DARTEL; Ashburner, 2007) with the template from 550 healthy controls of all ages in the

212 IXI Dataset (<http://www.brain-development.org>) in MNI space. We then applied a 12-
213 parameter affine registration and nonlinear transformation to correct for image size and
214 position. The voxel size was resampled to $1.5 \times 1.5 \times 1.5$ mm and smoothed using a 8-mm
215 Gaussian kernel. For each subject, whole-brain gray matter volume (GMV) was calculated.
216 An absolute threshold mask of 0.05 was specified in the analyses to cover the whole brain.
217 For quality assessment, we visually inspected the segmentation quality and image
218 homogeneity with the CAT12 toolbox. One participant from the middle-aged group was
219 excluded because of MRI inhomogeneities.

220 *Functional MRI.* Preprocessing was implemented in Nipype (Gorgolewski et al.,
221 2011), incorporating tools from FreeSurfer (Fischl, 2012), FSL (Jenkinson et al., 2012), AFNI
222 (Cox, 1996), ANTs (Avants et al., 2011), CBS Tools (Bazin et al., 2014), and Nitime (Rokem
223 et al., 2009). The pipeline comprised the following steps: (I) discarding the first five EPI
224 volumes to allow for signal equilibration and steady state, (II) 3D motion correction (FSL
225 mcflirt), (III) distortion correction (FSL fugue), (IV) rigid body co-registration of functional
226 scans to the individual T1-weighted image (Freesurfer bbregister), (V) denoising including
227 removal of 24 motion parameters (CPAC, Friston et al., 1996), motion, signal intensity spikes
228 (Nipype rapidart), physiological noise in white matter and cerebrospinal fluid (CSF)
229 (CompCor; Behzadi et al., 2007), together with linear and quadratic signal trends, (VI) band-
230 pass filtering between 0.01-0.1 Hz (Nilearn), (VII) spatial normalization to MNI152 standard
231 space (3 mm isotropic) via transformation parameters derived during structural preprocessing
232 (ANTs). (VIII) The data were then spatially smoothed with a 6-mm FWHM Gaussian kernel.

233 The reproducible workflows containing all implementation details for our datasets can
234 be found here: LIFE; https://github.com/fliem/LIFE_RS_preprocessing, LEMON;
235 <https://github.com/NeuroanatomyAndConnectivity/pipelines/releases/tag/v2.0>

236 *Eigenvector Centrality Mapping (ECM)*. In ECM, each voxel in the brain receives a
237 centrality value that is larger if the voxel is strongly correlated with many other voxels that
238 are themselves central (Lohmann et al., 2010). ECM is computationally efficient, enables
239 connectivity analysis at the voxel level, and does not require initial thresholding of
240 connections (Lohmann et al., 2010). Here, the fast ECM implementation was used (Wink et
241 al., 2012). We restricted our ECM analysis to GM, which we extracted with a mask from the
242 tissue priors in SPM12 by selecting voxels with a GM tissue probability of 20% or higher.
243 The resulting mask contained ~63,000 voxels covering the entire brain.

244 *Exploratory Seed-based Functional Connectivity Analysis (SBCA)*. To further explore
245 the connectivity patterns of significant centrality changes across the whole brain, ECM was
246 complemented by SBCA. Regions detected in ECM can be used as seeds in a subsequent
247 SBCA to investigate intrinsic functional connectivity patterns (Taubert et al., 2011). A
248 bilateral vmPFC seed was created by binarizing the significant ECM findings (MNI
249 coordinates: [x=0, y=57, z=-6], cluster size k=62). Time series were extracted and averaged
250 across all voxels of the seed. For each subject, a correlation between the time series of the
251 seed and every other voxel in the brain was calculated using 3dfim+ (AFNI). The resulting
252 correlation maps were Fisher r-to-z transformed using 3dcalc (AFNI).

253 *Statistical analyses*. Statistical analyses were carried out using the general linear model
254 (GLM) approach implemented in SPM12. We performed one-way ANOVA with three age
255 groups (young, middle, and old) as between-subjects factor together with HRV as the variable
256 of interest and age, sex, study, and either total intracranial volume (TIV, for VBM analysis) or
257 in-scanner head motion (mean FD; Power et al., 2012 for ECM and SBCA) as covariates of
258 no interest.

259 We first calculated the interaction effect between HRV and age group. Based on the
260 significant results of the ANOVA, we computed pairwise group differences using

261 independent t-tests. Using one-sample t-tests, we further tested the main effect of HRV across
262 all subjects, as well as for each age group separately. For each statistical analysis, a positive
263 and a negative contrast were computed. Only results surviving whole-brain family-wise error
264 (FWE) correction at $p < 0.05$ (cluster-level) with a voxel-level threshold of $p < 0.001$ were
265 considered significant. All (unthresholded) statistical maps are available at NeuroVault
266 (Gorgolewski et al., 2015) for detailed inspection in 3D
267 (<http://neurovault.org/collections/TELEUIIY>).

268 2.5. Cognitive measurement and potential confounding factors for HRV

269 *Sex.* As HRV has been reported to differ between sexes (Koenig and Thayer, 2016;
270 Voss et al., 2015), we analyzed sex differences in HRV per age group in a 2 (sex) \times 3 (age
271 group) ANOVA.

272 *Smoking.* Since smoking has a short- and long-term impact on HRV (Felber Dietrich
273 et al., 2007; Hayano et al., 1990), we examined potential effects of smoking status on HRV.
274 To this end, we classified subjects into three groups (smokers: N= 75, former smokers: N=84,
275 and non-smokers: N=220, [no info available: NA=9]). We used a 2 (sex) \times 3 (smoking)
276 ANOVA to test the mean differences between the groups using sex as additional between-
277 subjects factor.

278 *Cognition.* The Trail Making Test (TMT) is a cognitive test measuring executive
279 function, including processing speed and mental flexibility. By drawing lines, subjects
280 sequentially connect numbers and/or letters while their reaction times are recorded (Reitan,
281 1955; Reitan and Wolfson, 1995). In the first part of the test (TMT-A) the targets are all
282 numbers (1, 2, 3, etc.), while in the second part (TMT-B), participants need to alternate
283 between numbers and letters (1, A, 2, B, etc.). In both TMT A and B, the time to complete the
284 task quantifies the performance and lower scores indicate better performance.

285 *Blood Pressure.* Systolic blood pressure (SBP) and diastolic blood pressure (DBP) were

286 measured in a seated position using an automatic oscillometric blood pressure monitor (LIFE
287 sample; OMRON 705IT, LEMON sample; OMRON M500) after a resting period of 5 min.
288 While in the LIFE sample three consecutive blood pressure measurements were taken from
289 the right arm in intervals of 3 minutes, in the LEMON sample measurements were taken from
290 participants' left arms on three separate occasions within two weeks. In each sample, all
291 available measurements per participant were averaged to one systolic and one diastolic blood
292 pressure value.

293 *Anthropometric measurements.* Subjects' heights and weights were taken according to a
294 standardized protocol by trained study staff. Body mass index (BMI; in kg/m²) was calculated
295 by dividing the body weight by the square of the body height, while waist to hip ratio (WHR)
296 was calculated as waist circumference measurement divided by hip circumference
297 measurement (Huxley et al., 2010). As a control, all analyses on the association between HRV
298 and the brain across the age groups were repeated with blood pressure (BP) and body mass
299 index (BMI) as additional covariates of no interest.

300 For cognition, blood pressure, and anthropometric measurements, we assessed age-group
301 differences statistically using one-way ANOVAs, and then tested their association with HRV
302 using Spearman correlations for each age group. To determine statistical significance, we
303 used a two-sided α -level of 0.05. Statistical analyses were conducted using R version 3.3.2 (R
304 Core Team 2016).

305

3. Results

306

Details about the demographic, anthropometric, cardiovascular, and cognitive

307

characteristics of the 388 participants can be found in Table 1. The age groups differed

308

significantly in all variables (Table 1).

309

Table 1. Participant characteristics for each age group. For continuous variables, data is

310

provided in means and standard deviations (in parenthesis). One-way ANOVAs were used to

311

detect age group differences.

	Young (20-35 years) (N=140)	Middle (35-60 years) (N=119)	Old (60-80 years) (N=129)	df	F-value	Eta- squared (η^2)
Age	26.01 (4.17)	46.39 (6.25)	66.88 (4.68)			
Sex	38 M / 102 F	36 M / 83 F	50 M / 79 F		4.38‡	
Resting HRV (RMSSD in ms)	53 (27.11)	32.77 (21.01)	27.27 (22.99)	385	43.01***	0.182
Mean HR (1/min)	64.38 (9.62)	62.93 (10.01)	66.24 (10.44)	385	3.411*	0.017
RR interval (ms)	952.56 (137.06)	977.87 (149.75)	928.32 (148.53)	385	3.62*	0.018
mean FD (mm)	0.18 (0.05)	0.28 (0.10)	0.31 (0.11)	385	82.61***	0.300
BMI (kg/m ²)	23.58 (3.03)	26.51 (3.62)	26.54 (3.57)	382	33.34***	0.148
WHR	0.86 (0.07)	0.92 (0.08)	0.95 (0.08)	381	47.64***	0.200
SBP (mmHg)	122.08 (11.42)	126.55 (13.74)	138.76 (18.2)	381	45.45***	0.192
DBP (mmHg)	71.23 (7.33)	78.21 (9.11)	80.00 (10.44)	381	35.47***	0.156
TMT A (s)	24.95 (7.79)	30.33 (12.73)	40.01 (13.54)	384	58.48***	0.233
TMT B (s)	57.72 (17.89)	71.40 (39.04)	95.15 (45.09)	382	45.73***	0.193

312 * $p < 0.05$; ** $p < 0.01$; *** $p < 0.001$, 2-tailed

313 ‡ Kruskal-Wallis-Test

314 *Note.* HRV = heart rate variability; RMSSD = root mean square of successive differences; HR
315 = heart rate, FD = framewise displacement; BMI = body mass index; WHR = waist to hip
316 ratio; SBP = systolic blood pressure; DBP = diastolic blood pressure; TMT = trail making
317 test.

318

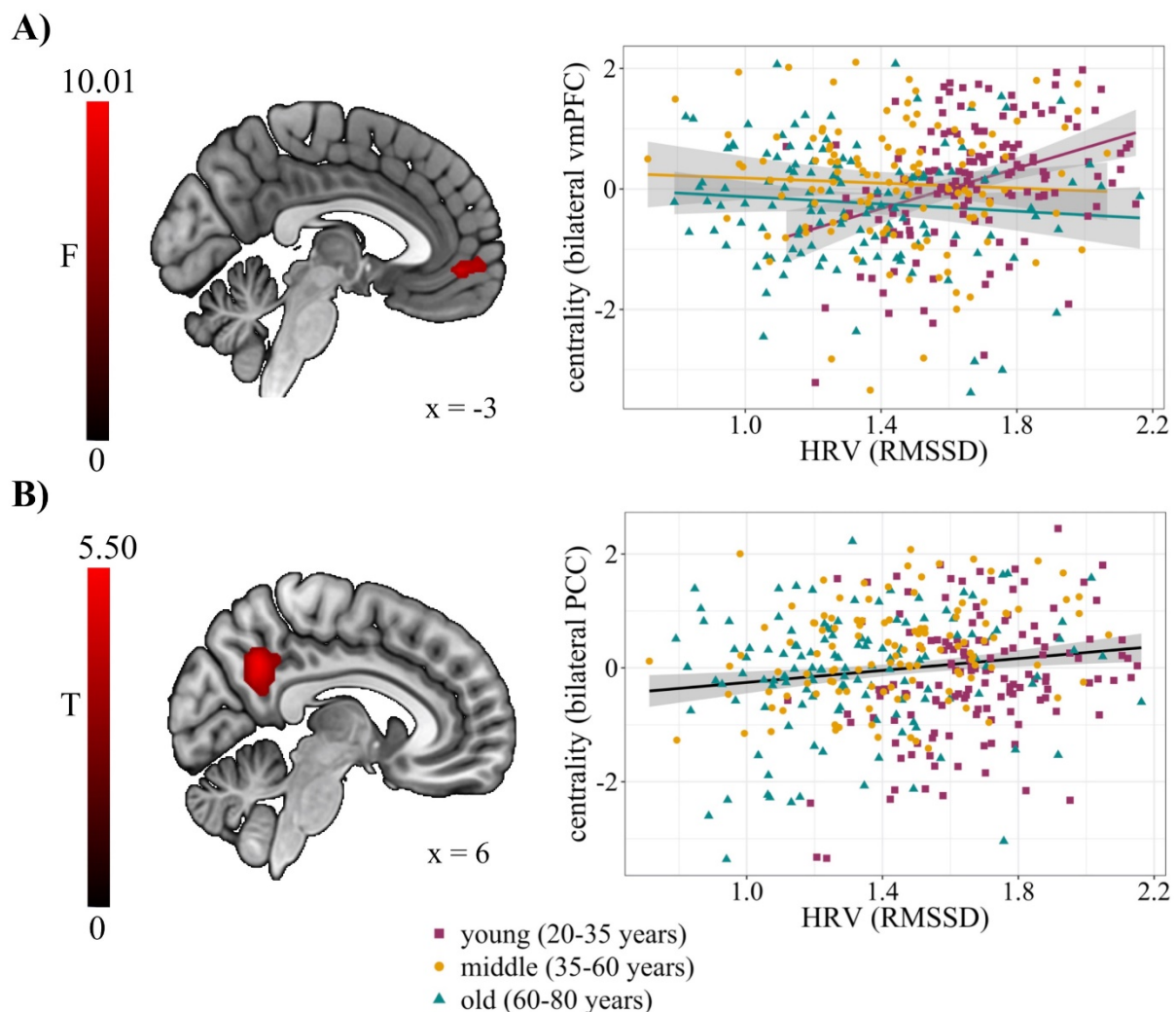
319 There was a significant main effect of age group on HRV ($F(2,382) = 63.552$, $p = 2 \times 10^{-16}$, $\eta^2 = 0.182$), sex did not show a significant main effect on HRV ($F(1,382) = 0.187$, $p =$
320 0.666), and there was no significant age group \times sex interaction on HRV ($F(2,382) = 0.233$, $p =$
321 0.792). HRVs of smokers, former smokers, and non-smokers did not differ significantly
322 from each other (main effect smoking group: $F(2,373) = 1.241$, $p = 0.290$, main effect of sex:
323 $F(1,373) = 0.473$, $p = 0.492$; smoking group \times sex interaction: $F(2,373) = 0.606$, $p = 0.546$).

324 HRV was negatively correlated with age ($\rho = -0.21$, $p = 0.010$), BMI ($\rho = -0.207$, $p =$
325 0.020), and DBP ($\rho = -0.231$, $p = 0.012$) within the middle-aged individuals. No
326 significant associations were found between HRV and mean FD, SBP, WHR, TMT A, and
327 TMT B in any of the age groups (Supplementary Table 1).

328 *Voxel-based Morphometry (VBM).* There was no significant association between HRV
329 and GMV across all subjects. Also, an ANOVA did not yield a significant age group \times HRV
330 interaction on GMV. While an exploratory one-sample t-test in the middle-aged group
331 indicated a significant HRV-related increase of GMV in left cerebellum (MNI coordinates: [-
332 15, -87, -51], $k = 1540$, $T = 3.92$, $p_{\text{FWE}} = 0.004$), there were no significant effects of HRV on
333 GMV for younger and older adults. Control analyses that included BP and BMI as covariates
334 of no interest did not change the results.

336 *Eigenvector Centrality Mapping (ECM)*. A significant effect of age group on the
337 relation between resting HRV and EC was detected in the bilateral vmPFC (MNI coordinates:
338 [0, 57, -6], $k = 62$, $F = 10.79$). The beta values from bilateral vmPFC for each age group are
339 plotted in Figure 1A, suggesting that younger adults show a stronger association between
340 HRV and EC in bilateral vmPFC than middle-aged and older individuals (Table 2). This was
341 supported by post-hoc two-sample t-tests, which indicated that the correlation between HRV
342 and EC in bilateral vmPFC was significantly stronger for the contrasts of young > old and
343 young > middle-age (Table 2). A one-sample t-test across all subjects showed increased EC
344 with higher HRV in bilateral PCC (Figure 1B). The negative contrast did not yield any
345 significant results. In separate one-sample t-tests for each age group, we found HRV-
346 dependent EC increases in right vmPFC, bilateral PCC, and superior frontal gyrus (SFG), as
347 well as HRV-dependent EC decreases in left superior occipital gyrus (SOG) including cuneus
348 and calcarine sulcus in the group of young subjects. Our data did not show any significant
349 positive or negative correlation with HRV in the groups of middle-aged and old subjects that
350 were correctable for multiple comparisons. The complete ECM results are presented in Table
351 2. Control analyses that included BP and BMI as covariates of no interest did not change the
352 results.

353 **Fig. 1.** Association between resting heart rate variability (HRV), measured as root mean square
354 of successive differences (RMSSD), and eigenvector centrality (EC). **A)** The interaction
355 between age group and HRV was significant in the bilateral ventromedial prefrontal cortex
356 (vmPFC; MNI coordinates: [0, 57, -6], $k = 62$, $F = 10.79$, $p_{FWE} = 0.006$), displayed at $x = -3$.
357 **B)** An increased EC in the bilateral posterior cingulate cortex (PCC; MNI coordinates [6, -54,
358 36], $k = 204$, $T = 5.29$, $p_{FWE} < 0.001$) across all age groups, displayed at $x = 6$. Results are
359 shown at a voxel threshold of $p < 0.001$ with family-wise error (FWE) correction with $p < 0.05$
360 at the cluster level.



361

362 **Table 2.** Brain regions that show significant increases or decreases in eigenvector centrality
 363 with heart rate variability (HRV). Thresholds: $p < 0.001$ at the voxel and $p < 0.05$ with
 364 family-wise error (FWE) correction at the cluster level.

	Regions	H	cluster size k (Voxel)	MNI coordinates			FWE	z	F/T- value
				x	y	z			
ANOVA	Ventromedial prefrontal cortex	R/L	62	0	57	-6	0.006	4.03	10.79
				-3	48	-6		3.76	9.63
				0	60	3		3.49	8.53
Across age groups (+)	Posterior cingulate cortex /precuneus	R/L	204	6	-54	36	<0.001	5.29	5.39
				-9	-57	33		4.04	4.09
				-12	-51	45		3.35	3.38
Young (+)	Ventromedial prefrontal cortex	R	316	0	57	-6	<0.001	5.07	5.16
				6	51	9		4.89	4.98
				15	60	15		4.22	4.16
	Posterior cingulate cortex /precuneus	R/L	167	6	-57	27	<0.001	4.46	4.52
				-9	-54	18		3.72	3.75
				-9	-60	27		3.70	3.74
Superior frontal gyrus	R/L	240	15	33	48	0.002	4.50	4.56	
			15	48	39		4.32	4.37	
			-6	36	48		4.24	4.29	
Young (-)	Superior occipital gyrus	L	129	-6	-96	3	<0.001	4.63	4.70
				-15	-99	-3		4.24	4.29
				0	-84	-3		3.71	3.76
Middle (+)	n.s								
Middle (-)	n.s								
Old (+)	n.s								
Old (-)	n.s								
Young > Old	Ventromedial prefrontal cortex	R	131	0	57	-6	<0.001	4.45	4.51
				0	60	3		4.01	4.05
				-3	45	-8		3.62	3.65
Young < Old	n.s								
Middle > Young	n.s								
Middle < Young	Ventromedial prefrontal cortex	R	85	3	45	-6	0.005	4.09	4.13
				-12	48	-9		4.06	4.11
				6	45	15		3.58	3.61
Old > Middle	n.s								
Old < Middle	n.s								

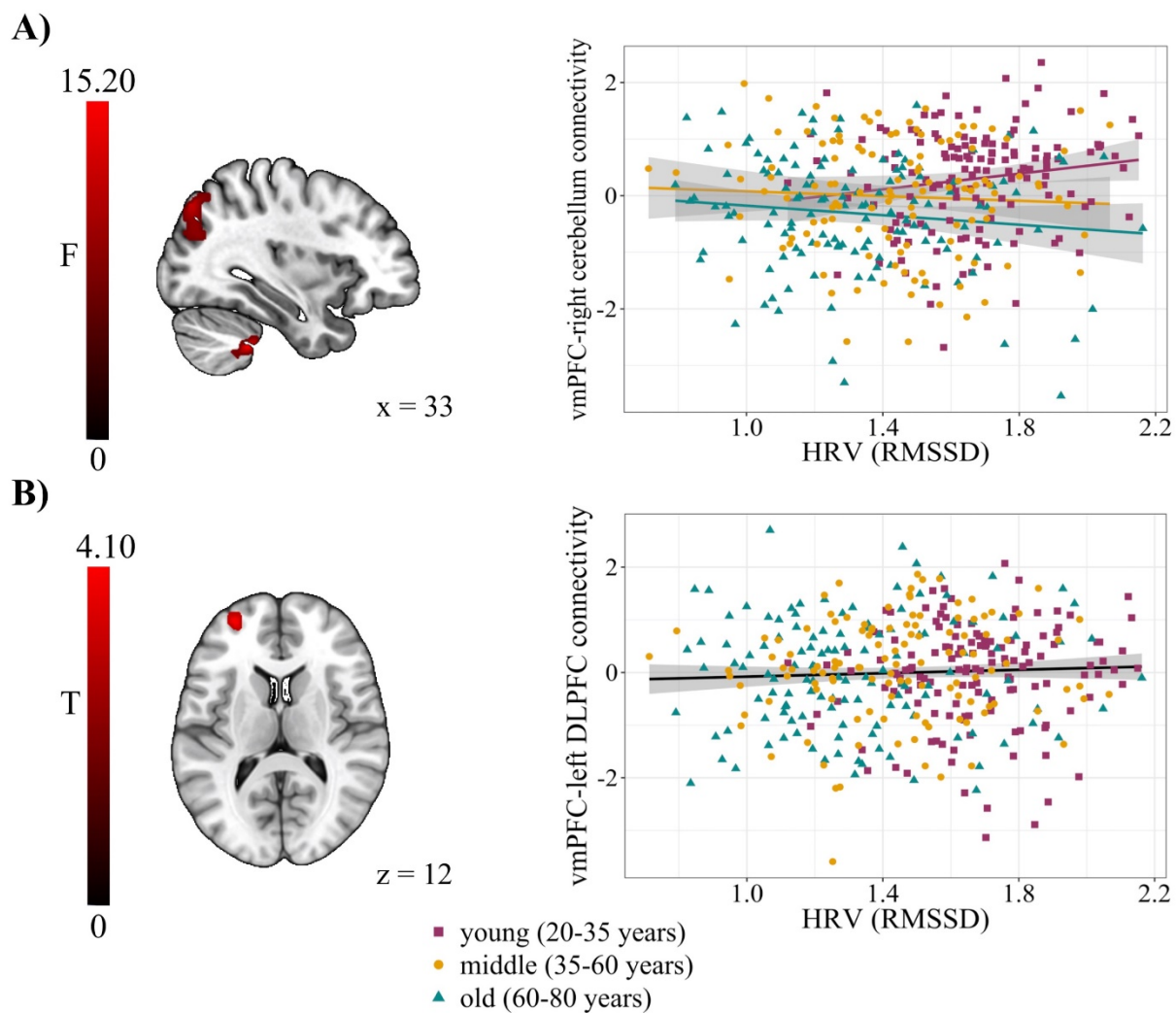
365 *Note.* R= right, L = left, H = hemisphere, ANOVA = analysis of variance, MNI = Montreal
366 Neurological Institute, n.s = not significant

367

368 *Exploratory Seed-based Functional Connectivity Analysis (SBCA).* In the additional
369 exploratory seed-based functional connectivity analysis, a significant effect of age group on
370 the relation between resting HRV and whole-brain bilateral vmPFC connectivity was found in
371 bilateral cerebellum, right superior parietal lobe (SPL), left middle occipital gyrus (MOG) and
372 inferior occipital gyrus (IOG), and left SFG extended to supplementary motor area (SMA).
373 The beta values from the right cerebellum for each age group are plotted in Figure 2A,
374 suggesting that younger adults show stronger functional connectivity between bilateral
375 vmPFC and right cerebellum than middle-aged and older individuals (Table 3). The post-hoc
376 two-sample t-tests similarly indicated that higher HRV levels were significantly correlated
377 with stronger functional connectivity between bilateral vmPFC and bilateral cerebellum, right
378 SPL, left MOG, left post-central gyrus, and left SMA for the contrasts of young > old and
379 young > middle (Table 3). A one-sample t-test in the overall sample, to assess the association
380 between HRV and bilateral vmPFC connectivity, showed an increased functional connectivity
381 with left middle frontal gyrus (MFG) extending to dorsolateral prefrontal cortex (DLPFC)
382 (Figure 2B). Separate one-sample t-tests for each age group showed no significant association
383 for the middle-aged and old subjects but an increased vmPFC connectivity in distributed brain
384 regions including bilateral cerebellum, bilateral MOG, and right SMA for the young subjects.
385 We did not observe any significant negative correlations neither in the overall sample nor in
386 each age group. Control analyses that included BP and BMI as covariates of no interest did
387 not change the results. The complete SBCA results are presented in Table 3.

388

389 **Fig. 2.** Association between resting heart rate variability (HRV), measured as root mean square
390 of successive differences (RMSSD), and brain function in an exploratory seed-based functional
391 connectivity analysis originating from bilateral ventromedial prefrontal cortex (vmPFC). **A)**
392 The interaction between age group and HRV was significant in the right cerebellum (MNI
393 coordinates [33, -42, -45], $k = 46$, $F = 15.19$, $p_{FWE} < 0.001$), displayed at $x = 33$. **B)** An
394 increased functional connectivity in the right dorsolateral prefrontal cortex (DLPFC; MNI
395 coordinates [-30, 54, 12], $k = 67$, $T = 4.10$, $p_{FWE} = 0.032$) was found across all age groups,
396 displayed at $z = 12$. Results are shown at a voxel threshold of $p < 0.001$ with family-wise error
397 (FWE) correction with $p < 0.05$ at the cluster level.



399 **Table 3.** Brain regions that show resting heart rate variability-related connectivity with the
 400 bilateral ventromedial prefrontal cortex (vmPFC) in an exploratory seed-based functional
 401 connectivity analysis. Thresholds: $p < 0.001$ at the voxel and $p < 0.05$ with family-wise error
 402 (FWE) correction at the cluster level.

	Regions	H	cluster size k (Voxels)	MNI coordinates			FWE	z	F/T-value
				x	y	z			
ANOVA	Cerebellum	R	46	33	-42	-45	0.049	4.91	15.19
	Superior parietal lobe	R	203	24	-75	51	<0.001	4.48	12.94
				33	-78	45		4.34	12.25
				36	-75	30		3.82	9.88
	Middle occipital gyrus	L	57	-33	-84	30	0.021	4.24	11.74
				-39	-66	24		3.31	7.84
	Inferior occipital gyrus		60	-33	-69	-6	0.016	3.85	9.97
				-42	-63	-3		3.76	9.61
				-51	-69	-15		3.62	9.03
	Cerebellum	L	61	-30	-60	-30	0.015	3.83	9.91
-33				-66	-21	3.59		8.91	
-39				-72	-18	3.58		8.87	
Superior frontal gyrus extended to supplementary motor area	L	71	0	15	66	0.007	3.73	9.47	
			0	3	57		3.6	8.96	
			9	12	57		3.53	8.66	
Across age groups (+)	Middle frontal gyrus extended to dorsolateral prefrontal cortex	L	67	-30	54	12	0.032	4.06	4.10
				-36	54	3		3.54	3.57
				-18	51	3		3.39	3.42
Young (+)	Cerebellum	R	131	33	-42	-45	0.001	5.06	5.15
				42	-60	-48		4.68	4.75
				36	-63	-39		3.29	3.31

	Cerebellum	L	116	-12	-57	-54	0.002	4.6	4.67
				-21	-69	-54		4.2	4.25
				-15	-48	-51		4.09	4.14
	Middle occipital gyrus		163	39	-75	42	<0.001	4.46	4.52
		R		30	-69	51		4.15	4.20
				21	-78	51		3.63	3.67
	Middle occipital gyrus		131	-39	-66	24	0.001	4.31	4.37
		L		-33	-84	30		3.94	3.98
				-39	-60	12		3.47	3.50
	Cerebellum	R	63	18	-75	-18	0.04	4.13	4.18
				27	-81	-18		3.68	3.72
				18	-84	-15		3.64	3.67
	Cerebellum	L	102	-33	-81	-21	0.005	4.13	4.18
				-30	-60	-30		3.7	3.74
				-21	-90	-15		3.59	3.62
	Supplementary motor area	R	87	3	6	54	0.01	3.77	3.81
				0	15	69		3.68	3.72
				9	12	57		3.59	3.63
Young (-)	n.s								
Middle (+)	n.s								
Middle (-)	n.s								
Old (+)	n.s								
Old (-)	n.s								
Young > Old	Cerebellum	R	67	33	-42	-45	0.032	4.59	4.66
				15	-48	-51		3.63	3.67
				27	-57	-45		3.41	3.44
	Inferior occipital gyrus	L	237	-33	-69	-6	<0.001	4.41	4.47
				-42	-63	-3		4.33	4.38
				-39	-72	-18		4.14	4.19

	Superior parietal lobe	R	275	24	-78	51	<0.001	4.31	4.37
				36	-75	45		4.21	4.26
				36	-75	27		3.95	4
	Middle occipital gyrus	L	140	-27	-84	27	0.001	4.30	4.35
				-36	-66	24		3.89	3.93
				-39	-60	12		3.62	3.65
	Superior frontal gyrus extended to supplementary motor area	L	147	-3	3	57	0.001	3.99	4.04
				12	6	63		3.72	3.75
				3	12	66		3.61	3.65
	Postcentral gyrus	R	72	42	-6	30	0.024	3.87	3.91
				54	6	24		3.69	3.73
				54	0	33		3.53	3.56
	Superior frontal gyrus extended to supplementary motor area	R	73	3	-18	60	0.022	3.62	3.66
				-3	-36	69		3.56	3.59
				3	-9	69		3.29	3.31
Young < Old	n.s								
Middle > Young	n.s								
Middle < Young	Cerebellum	R	189	33	-42	-45	<0.001	4.99	5.08
				42	-60	-48		4.60	4.67
				18	-45	-51		4.34	4.40
	Superior parietal lobe	R	270	27	-72	51	<0.001	4.76	4.83
				33	-78	45		4.51	4.58
				36	-75	30		4.04	4.09
	Cerebellum	L	239	-12	-57	-54	<0.001	4.74	4.82
				-15	-45	-51		4.61	4.68
				-12	-39	-45		4.36	4.42
	Middle occipital gyrus	L	76	-33	-84	30	0.019	4.59	4.66
				-45	-72	27		3.37	3.40

	Cerebellum	L	313	-30	-60	-30	<0.001	4.27	4.32
				12	-69	-21		4.18	4.23
				18	-78	-18		3.95	3.99
	Superior frontal gyrus extended to supplementary motor Area	L	109	0	15	66	0.003	4.19	4.24
				15	9	69		3.61	3.64
	Old > Middle		n.s						
	Old < Middle		n.s						

403 *Note.* R= right, L = left, H = hemisphere, ANOVA = analysis of variance, MNI = Montreal

404 Neurological Institute

405 4. Discussion

406 In the present study, we assessed the relationship between parasympathetic
407 cardiorespiration (using resting HRV) and brain structure (using VBM) as well as whole-brain
408 resting-state connectivity (using ECM and SBCA) in a large sample of healthy young,
409 middle-aged, and old participants. We found the frequently observed age-related decrease in
410 resting HRV (Almeida-Santos et al., 2016; Voss et al., 2015) to be accompanied by alterations
411 in brain function. Specifically, higher HRV was linked to stronger network centrality in
412 several brain regions, particularly along the cortical midline. In the PCC, this correlation was
413 present in all age groups while in the vmPFC, network centrality was related to higher HRV
414 in young but not in middle-aged and old adults. These findings support the view that altered
415 HRV during aging may have a functional brain component associated with it.

416 4.1. Age-dependent association of resting HRV with functional connectivity

417 Given the relationship between HRV and age (Almeida-Santos et al., 2016; Voss et
418 al., 2015), HRV and brain structure (Wei et al., 2018), as well as HRV and brain function
419 (Sakaki et al., 2016), we hypothesized the neural correlates of resting HRV to be also age-
420 dependent. Our results confirm that the relationship between HRV and network centrality at
421 rest differs between age groups. Evidence is accumulating that alterations of intrinsic brain
422 activity are a key feature of normal brain aging (Damoiseaux et al., 2008): age-dependent
423 intrinsic connectivity alterations in the DMN have been found not only in healthy aging
424 (Ferreira and Busatto, 2013) but also in (age-related) pathologies, for example, in individuals
425 with a high familial risk for depression (Posner et al., 2016) and in young APOE-ε4 carriers
426 (Filippini et al., 2009), which is a possible biomarker for Alzheimer's dementia (Kanekiyo et
427 al., 2014). Our results that resting HRV is related to increased network centrality in medial
428 frontal regions in the young but not in the middle-aged and old age group could be interpreted
429 in the framework of the functional plasticity hypothesis of cognitive aging (Greenwood,

430 2007). According to this hypothesis, the structural vulnerability particularly of prefrontal
431 cortex leads to an age-related functional reorganization (e.g., Grady, 2012; for a detailed
432 review). Changes in the resting-state network architecture around the vmPFC that are related
433 to parasympathetic cardiorespiration could thus represent altered cardiovascular control with
434 advancing age and concomitant network reorganization.

435 In addition to the age-dependent association of resting HRV with functional brain
436 network centrality in medial frontal regions, we also found an HRV-related bilateral medial
437 parietal cluster in the PCC that was independent of age. Both vmPFC and PCC are central
438 nodes of the DMN (Greicius et al., 2003; Uddin et al., 2009) and have been related to self-
439 generated or internally directed mental processes like thoughts and feelings (Andrews-Hanna
440 et al., 2014; Raichle et al., 2001). Regions of the DMN – and particularly its medial frontal
441 (e.g., vmPFC) and parietal components (e.g., PCC and precuneus) – have also been implied in
442 the central processing of autonomic – and particularly parasympathetic – function (Beissner et
443 al., 2013; Benarroch, 1993). It is plausible that in the absence of external stimulation, brain
444 function (i.e., activity and connectivity) is predominantly allocated to the “internal milieu”,
445 that is, to monitoring and regulating bodily signals (e.g., the parasympathetic “rest-and-
446 digest”). Fittingly, the PCC has been found active in tasks that involved the assessment of
447 self-relevance (Yu et al., 2011) as well as self-location and body ownership (Guterstam et al.,
448 2015), while the vmPFC was related to processing bodily information (Gusnard et al., 2001),
449 autonomic control (Critchley et al., 2011), and cardiovascular arousal (Wong et al., 2007).
450 Similarly, a causal role of the PFC for cardiovascular activity (e.g., HR and HRV) was found
451 in a meta-analysis of non-invasive brain stimulation and autonomic functioning (Makovac et
452 al., 2017).

453 The exploratory SBCA similarly showed an age-dependent relationship between
454 resting HRV and functional brain connectivity. Specifically, we found stronger functional

455 connectivity between bilateral vmPFC and a widespread set of brain regions including
456 bilateral cerebellum, occipital gyrus, right SPL, and SFG extending to SMA in young but not
457 middle-aged and old adults. These results extend the ECM findings by suggesting additional
458 cortico-cerebellar regions might be involved in the modulation of visceral processes. In line
459 with this interpretation, activation in the cerebellum has been connected to the regulation of
460 visceral responses (Demirtas-Tatlidede et al., 2011), fear conditioning (Leaton, 2003;
461 Sacchetti et al., 2002), feeding (Tataranni et al., 1999), as well as the coordination and control
462 of cardiovascular activities (Bradley et al., 1991; Ghelarducci and Sebastiani, 1996).
463 Furthermore, autonomic activity during cognitive and motor tasks was positively associated
464 with activation in the cerebellum and, among other regions, the SMA and dorsal ACC
465 (Critchley et al., 2003).

466 Despite previous evidence of the relationship between brain structure and vagally-
467 mediated HRV in central autonomic network regions (Wei et al., 2018), using whole-brain
468 VBM analysis, we only found a significant GMV change related with resting HRV in the
469 cerebellum for the middle-aged group. Notably, in the study by Wei et al. (2018) reduced GM
470 volume in the cerebellum was associated with HR (but not HRV) in healthy middle-aged
471 individuals. The divergent results could be due to different measurement parameters (e.g.,
472 MRI sequence parameters) but also to different effect size and statistical power (for more
473 details see *Limitations*).

474 4.2. Physiological and psychophysiological interpretations of HRV

475 The most fundamental (purely physiological) understanding of the role of the ANS –
476 and particularly the PNS – is to ensure visceral and cardiovascular functioning or bodily
477 homeostasis – by allowing rapid adaptive behavioral and physiological reactions in ever-
478 changing environments or by disengagement and relaxation in resting moments (“rest-and-
479 digest”; e.g., Cannon, 1929).

480 More *psychophysiological* interpretations of ANS function have extended this view to
481 cognitive, affective, and social phenomena: For example, the two main theoretical
482 perspectives of HRV – the polyvagal theory (Porges, 2007, 2001, 1995) and the neurovisceral
483 integration model (Smith et al., 2017; Thayer and Lane, 2000; Thayer and Ruiz-Padial, 2006)
484 – suggest that PNS activation can serve as a biomarker of what can be summarized as “top-
485 down” self-regulation (Holzman and Bridgett, 2017). The polyvagal theory (Porges, 2007)
486 takes an evolutionary approach, according to which the role of the ANS and particularly the
487 vagus nerve can be understood as increasing adaptability through socially engaged behaviors
488 (e.g., self-soothing) and inhibition of sympathetic-adrenal influences on the body (Porges,
489 2007). The neurovisceral integration model (Smith et al., 2017; Thayer and Lane, 2000;
490 Thayer and Ruiz-Padial, 2006) highlights the role of vagally-mediated HRV for emotional or
491 self-regulation. This model explicitly links the brain and the rest of the body by assuming that
492 the PFC – and particularly the vmPFC – tonically inhibits the amygdala, which affects
493 autonomic function, thereby linking both nervous systems to inhibitory or (self-)regulatory
494 processes (Kemp et al., 2017; Thayer et al., 2012). Convergently, resting HRV has recently
495 been associated with vmPFC activation during a dietary self-control task in young adults
496 (Maier and Hare, 2017). Both theories draw on evidence that higher HRV is indicative of
497 better bodily functioning by enabling physiological and behavioral adaptation through
498 cognitive and socio-emotional flexibility. Taken together, our findings are consistent with
499 both the polyvagal theory and the neurovisceral integration model of HRV and extend them
500 by providing evidence for a brain network component of vagally-mediated HRV in healthy
501 aging.
502

503
504
505
506
507
508
509
510
511
512
513
514
515
516
517
518
519
520
521
522
523
524
525

5. Limitations

There are a number of limitations that should be considered in the interpretation of our results. The study design is cross-sectional and does not allow us to infer the directionality of the association between resting HRV and the brain. Additionally, our health criteria also allowed inclusion of subjects with higher BMI (>25 kg/m²) or untreated/undiagnosed hypertension (SBP > 140 mmHg, DBP > 90 mmHg). This makes it difficult to disentangle HRV-related influences from other bodily/cardiovascular influences – which are also physiologically related (BMI: Molino et al., 2009; BP: Singh et al., 1998). However, control analyses that accounted for BP and BMI showed very similar results of the association between resting HRV and the brain. Although psychological interpretations of a single physiological marker like resting HRV are intrinsically limited, previous studies have associated HRV with different trait or state levels of, for example, executive control (Capuana et al., 2014), stress (Sin et al., 2016), and emotion regulation (Williams et al., 2015). For a psychological interpretation of our finding that the association between HRV and functional connectivity at rest is age-dependent, similar analyses on task-related parasympathetic and neural activity could be helpful. Although we accounted for systematic study differences in the second-level GLM, different acquisition parameters of the rs-f/MRI and ECG may have influenced our results (e.g., for structural MRI; Streitbürger et al., 2014). Further, we calculated the RMSSD using 10 s of ECG data, which has been shown to be a valid measurement (Munoz et al., 2015; Nussinovitch et al., 2011a, 2011b). Nevertheless, ECG data recorded over longer periods (e.g., 24-hour) can complement this “ultra-short” evaluation of parasympathetic function.

526

6. Conclusion

527 In this cross-sectional study, we examined the association of resting HRV with brain
528 structure and functional brain connectivity in different age groups of healthy adults. Our main
529 findings are correlations between resting HRV and brain network architecture in the PCC
530 across all age groups and in the vmPFC in young but not in middle-aged and old subjects.
531 These support the view that the well-known HRV decrease with age may have a functional
532 brain network component along the cortical midline. Consistent with the role of these areas in
533 affective, cognitive, and autonomic regulation, our results provide a comprehensive picture of
534 the differential effect of age on heart-brain interactions and extend our knowledge of
535 parasympathetic cardioregulation being important for healthy aging.

536

7. Financial disclosures

537

The authors declare no conflict of interest

538

8. Acknowledgments

539 This study was supported by LIFE Leipzig Research Center for Civilization Diseases at
540 the University of Leipzig funded by the European Union, European Regional Development
541 Fund, and the Free State of Saxony. The authors would like to thank all volunteers for their
542 participation in one of the two studies. Further, we thank all researchers, technicians and
543 students who planned, collected, entered and curated data, used in this manuscript.

544

9. References

- 545 Almeida-Santos, M.A., Barreto-Filho, J.A., Oliveira, J.L.M., Reis, F.P., da Cunha Oliveira,
546 C.C., Sousa, A.C.S., 2016. Aging, heart rate variability and patterns of autonomic
547 regulation of the heart. *Arch. Gerontol. Geriatr.* 63, 1–8.
548 doi:10.1016/j.archger.2015.11.011
- 549 Andrews-Hanna, J.R., Smallwood, J., Spreng, R.N., 2014. The default network and self-
550 generated thought: Component processes, dynamic control, and clinical relevance. *Ann.*
551 *N. Y. Acad. Sci.* 1316, 29–52. doi:10.1111/nyas.12360
- 552 Arking, R., 2006. The biology of aging: observations and principles, *The Biology of Aging*
553 *Observations Principles.* doi:10.1080/03601270701498491
- 554 Ashburner, J., 2007. A fast diffeomorphic image registration algorithm. *Neuroimage* 38, 95–
555 113. doi:10.1016/j.neuroimage.2007.07.007
- 556 Ashburner, J., Friston, K.J., 2000. Voxel-Based Morphometry—The Methods. *Neuroimage*
557 11, 805–821. doi:10.1006/nimg.2000.0582
- 558 Avants, B.B., Tustison, N.J., Song, G., Cook, P.A., Klein, A., Gee, J.C., 2011. A reproducible
559 evaluation of ANTs similarity metric performance in brain image registration.
560 *Neuroimage* 54, 2033–2044. doi:10.1016/j.neuroimage.2010.09.025
- 561 Babayan, A., Erbey, M., Kumral, D., Reinelt, R. D., Reiter, A. M. F., Röbbig, J., Schaare, L.
562 H., Uhlig, M., ... Gaebler, M., Villringer, A., A Mind-Brain-Body dataset of MRI,
563 EEG, cognition, emotion, and peripheral physiology in young and old adults, under
564 review.
- 565 Bazin, P.L., Weiss, M., Dinse, J., Schäfer, A., Trampel, R., Turner, R., 2014. A computational
566 framework for ultra-high resolution cortical segmentation at 7 Tesla. *Neuroimage* 93,
567 201–209. doi:10.1016/j.neuroimage.2013.03.077
- 568 Behzadi, Y., Restom, K., Liau, J., Liu, T.T., 2007. A component based noise correction

- 569 method (CompCor) for BOLD and perfusion based fMRI. *Neuroimage* 37, 90–101.
570 doi:10.1016/j.neuroimage.2007.04.042
- 571 Beissner, F., Meissner, K., Bar, K.-J., Napadow, V., 2013. The Autonomic Brain: An
572 Activation Likelihood Estimation Meta-Analysis for Central Processing of Autonomic
573 Function. *J. Neurosci.* 33, 10503–10511. doi:10.1523/JNEUROSCI.1103-13.2013
- 574 Benarroch, E.E., 1993. The Central Autonomic Network: Functional Organization,
575 Dysfunction, and Perspective. *Mayo Clin. Proc.* 68, 988–1001. doi:10.1016/S0025-
576 6196(12)62272-1
- 577 Bradley, D.J., Ghelarducci, B., Spyer, K.M., 1991. The role of the posterior cerebellar vermis
578 in cardiovascular control. *Neurosci. Res.* 12, 45–56. doi:10.1016/0168-0102(91)90099-K
- 579 Buccelletti, E., Gilardi, E., Scaini, E., Galiuto, L., Persiani, R., Biondi, a, Basile, F., Silveri,
580 N.G., 2009. Heart rate variability and myocardial infarction: systematic literature review
581 and metanalysis. *Eur. Rev. Med. Pharmacol. Sci.* 13, 299–307.
- 582 Cannon, W.B., 1929. Organization for Physiological Homeostasis. *Physiol. Rev.* 9, 399–431.
583 doi:10.1152/physrev.1929.9.3.399
- 584 Capuana, L.J., Dywan, J., Tays, W.J., Elmers, J.L., Witherspoon, R., Segalowitz, S.J., 2014.
585 Factors influencing the role of cardiac autonomic regulation in the service of cognitive
586 control. *Biol. Psychol.* 102, 88–97. doi:10.1016/j.biopsycho.2014.07.015
- 587 Chang, C., Metzger, C.D., Glover, G.H., Duyn, J.H., Heinze, H.J., Walter, M., 2013.
588 Association between heart rate variability and fluctuations in resting-state functional
589 connectivity. *Neuroimage* 68, 93–104. doi:10.1016/j.neuroimage.2012.11.038
- 590 Cox, R.W., 1996. AFNI: Software for Analysis and Visualization of Functional Magnetic
591 Resonance Neuroimages. *Comput. Biomed. Res.* 29, 162–173.
592 doi:10.1006/cbmr.1996.0014
- 593 Critchley, H.D., Corfield, D.R., Chandler, M.P., Mathias, C.J., Dolan, R.J., 2000. Cerebral

594 correlates of autonomic cardiovascular arousal: a functional neuroimaging investigation
595 in humans. *J. Physiol.* 523 Pt 1, 259–270. doi:10.1111/j.1469-7793.2000.t01-1-00259.x
596 Critchley, H.D., Mathias, C.J., Josephs, O., O’Doherty, J., Zanini, S., Dewar, B.K., Cipolotti,
597 L., Shallice, T., Dolan, R.J., 2003. Human cingulate cortex and autonomic control:
598 Converging neuroimaging and clinical evidence. *Brain* 126, 2139–2152.
599 doi:10.1093/brain/awg216
600 Critchley, H.D., Nagai, Y., Gray, M.A., Mathias, C.J., 2011. Dissecting axes of autonomic
601 control in humans: Insights from neuroimaging. *Auton. Neurosci. Basic Clin.* 161, 34–
602 42. doi:10.1016/j.autneu.2010.09.005
603 Damoiseaux, J.S., Beckmann, C.F., Arigita, E.J.S., Barkhof, F., Scheltens, P., Stam, C.J.,
604 Smith, S.M., Rombouts, S.A.R.B., 2008. Reduced resting-state brain activity in the
605 “default network” in normal aging. *Cereb. Cortex* 18, 1856–1864.
606 doi:10.1093/cercor/bhm207
607 De Meersman, R.E., Stein, P.K., 2007. Vagal modulation and aging. *Biol. Psychol.* 74, 165–
608 173. doi:10.1016/j.biopsycho.2006.04.008
609 Demirtas-Tatlidede, A., Freitas, C., Pascual-Leone, A., Schmahmann, J.D., 2011. Modulatory
610 effects of theta burst stimulation on cerebellar nonsomatic functions. *Cerebellum* 10,
611 495–503. doi:10.1007/s12311-010-0230-5
612 Felber Dietrich, D., Schwartz, J., Schindler, C., Gaspoz, J.-M., Barthélémy, J.-C., Tschopp, J.-
613 M., Roche, F., von Eckardstein, A., Brändli, O., Leuenberger, P., Gold, D.R.,
614 Ackermann-Liebrich, U., 2007. Effects of passive smoking on heart rate variability, heart
615 rate and blood pressure: an observational study. *Int. J. Epidemiol.* 36, 834–840.
616 doi:10.1093/ije/dym031
617 Ferreira, L.K., Busatto, G.F., 2013. Resting-state functional connectivity in normal brain
618 aging. *Neurosci. Biobehav. Rev.* 37, 384–400. doi:10.1016/j.neubiorev.2013.01.017

- 619 Filippini, N., MacIntosh, B.J., Hough, M.G., Goodwin, G.M., Frisoni, G.B., Smith, S.M.,
620 Matthews, P.M., Beckmann, C.F., Mackay, C.E., 2009. Distinct patterns of brain activity
621 in young carriers of the APOE- 4 allele. *Proc. Natl. Acad. Sci.* 106, 7209–7214.
622 doi:10.1073/pnas.0811879106
- 623 Fischl, B., 2012. FreeSurfer. *Neuroimage* 62, 774–781.
624 doi:10.1016/j.neuroimage.2012.01.021
- 625 Friston, K.J., Williams, S., Howard, R., Frackowiak, R.S.J., Turner, R., 1996. Movement-
626 related effects in fMRI time-series. *Magn. Reson. Med.* 35, 346–355.
627 doi:10.1002/mrm.1910350312
- 628 Ghelarducci, B., Sebastiani, L., 1996. Contribution of the cerebellar vermis to cardiovascular
629 control. *J. Auton. Nerv. Syst.* 56, 149–156. doi:10.1016/0165-1838(95)00068-2
- 630 Gianaros, P.J., Van Der Veen, F., Jennings, J.R., 2004. Regional cerebral blood flow
631 correlates with heart period and high-frequency heart period variability during working-
632 memory task: Implications for the cortical and subcortical regulation of cardiac
633 autonomic activity. *Psychophysiology* 41, 521–530. doi:10.1111/j.1469-
634 8986.2004.00179.x
- 635 Gorgolewski, K., Burns, C.D., Madison, C., Clark, D., Halchenko, Y.O., Waskom, M.L.,
636 Ghosh, S.S., 2011. Nipype: A Flexible, Lightweight and Extensible Neuroimaging Data
637 Processing Framework in Python. *Front. Neuroinform.* 5, 13.
638 doi:10.3389/fninf.2011.00013
- 639 Gorgolewski, K.J., Varoquaux, G., Rivera, G., Schwarz, Y., Ghosh, S.S., Maumet, C., Sochat,
640 V. V., Nichols, T.E., Poldrack, R.A., Poline, J.-B., Yarkoni, T., Margulies, D.S., 2015.
641 NeuroVault.org: a web-based repository for collecting and sharing unthresholded
642 statistical maps of the human brain. *Front. Neuroinform.* 9.
643 doi:10.3389/fninf.2015.00008

- 644 Grady, C., 2012. The cognitive neuroscience of ageing. *Nat. Rev. Neurosci.* 13, 491–505.
645 doi:10.1038/nrn3256
- 646 Greenwood, P.M., 2007. Functional Plasticity in Cognitive Aging: Review and Hypothesis.
647 *Neuropsychology* 21, 657–673. doi:10.1037/0894-4105.21.6.657
- 648 Greicius, M.D., Krasnow, B., Reiss, A.L., Menon, V., 2003. Functional connectivity in the
649 resting brain: A network analysis of the default mode hypothesis. *Proc. Natl. Acad. Sci.*
650 100, 253–258. doi:10.1073/pnas.0135058100
- 651 Griswold, M.A., Jakob, P.M., Heidemann, R.M., Nittka, M., Jellus, V., Wang, J., Kiefer, B.,
652 Haase, A., 2002. Generalized Autocalibrating Partially Parallel Acquisitions (GRAPPA).
653 *Magn. Reson. Med.* 47, 1202–1210. doi:10.1002/mrm.10171
- 654 Gusnard, D.A., Akbudak, E., Shulman, G.L., Raichle, M.E., 2001. Medial prefrontal cortex
655 and self-referential mental activity: Relation to a default mode of brain function. *Proc.*
656 *Natl. Acad. Sci.* 98, 4259–4264. doi:10.1073/pnas.071043098
- 657 Guterstam, A., Björnsdotter, M., Gentile, G., Ehrsson, H.H., 2015. Posterior cingulate cortex
658 integrates the senses of self-location and body ownership. *Curr. Biol.* 25, 1416–1425.
659 doi:10.1016/j.cub.2015.03.059
- 660 Hayano, J., Yamada, M., Sakakibara, Y., Fujinami, T., Yokoyama, K., Watanabe, Y., Takata,
661 K., 1990. Short- and long-term effects of cigarette smoking on heart rate variability. *Am.*
662 *J. Cardiol.* 65, 84–88. doi:10.1016/0002-9149(90)90030-5
- 663 Holzman, J.B., Bridgett, D.J., 2017. Heart rate variability indices as bio-markers of top-down
664 self-regulatory mechanisms: A meta-analytic review. *Neurosci. Biobehav. Rev.* 74, 233–
665 255. doi:10.1016/j.neubiorev.2016.12.032
- 666 Huxley, R., Mendis, S., Zheleznyakov, E., Reddy, S., Chan, J., 2010. Body mass index, waist
667 circumference and waist:hip ratio as predictors of cardiovascular risk: a review of the
668 literature. *Eur. J. Clin. Nutr.* 64, 16–22. doi:10.1038/ejcn.2009.68

- 669 Jenkinson, M., Beckmann, C.F., Behrens, T.E.J., Woolrich, M.W., Smith, S.M., 2012. Fsl.
670 Neuroimage 62, 782–790. doi:10.1016/j.neuroimage.2011.09.015
- 671 Jennings, J.R., Sheu, L.K., Kuan, D.C.H., Manuck, S.B., Gianaros, P.J., 2016. Resting state
672 connectivity of the medial prefrontal cortex covaries with individual differences in high-
673 frequency heart rate variability. Psychophysiology 53, 444–454. doi:10.1111/psyp.12586
- 674 Kanekiyo, T., Xu, H., Bu, G., 2014. ApoE and A β in Alzheimer’s disease: Accidental
675 encounters or partners? Neuron. doi:10.1016/j.neuron.2014.01.045
- 676 Kemp, A.H., Koenig, J., Thayer, J.F., 2017. From Psychological Moments to Mortality: A
677 Multidisciplinary Synthesis on Heart Rate Variability Spanning the Continuum of Time.
678 Neurosci. Biobehav. Rev. doi:10.1016/j.neubiorev.2017.09.006
- 679 Kemp, A.H., Quintana, D.S., 2013. The relationship between mental and physical health:
680 Insights from the study of heart rate variability. Int. J. Psychophysiol. 89, 288–296.
681 doi:10.1016/j.ijpsycho.2013.06.018
- 682 Kim, D.H., Lipsitz, L.A., Ferrucci, L., Varadhan, R., Guralnik, J.M., Carlson, M.C., Fleisher,
683 L.A., Fried, L.P., Chaves, P.H.M., 2006. Association between reduced heart rate
684 variability and cognitive impairment in older disabled women in the community:
685 Women’s Health and Aging Study I. J. Am. Geriatr. Soc. 54, 1751–1757.
686 doi:10.1111/j.1532-5415.2006.00940.x
- 687 Koenig, J., Thayer, J.F., 2016. Sex differences in healthy human heart rate variability: A
688 meta-analysis. Neurosci. Biobehav. Rev. 64, 288–310.
689 doi:10.1016/j.neubiorev.2016.03.007
- 690 Leaton, R., 2003. Fear and the cerebellum. Mol. Psychiatry 8, 461–462.
691 doi:10.1038/sj.mp.4001286
- 692 Liao, D., Cai, J., Rosamond, W., Barnes, R., Hutchinson, R., Whitsel, E., Rautaharju, P.,
693 Heiss, G., 1997. Cardiac Autonomic Function and Incident Coronary Heart Disease: A

- 694 Population-based Case-Cohort Study The ARIC Study. *Am. J. ...* 145, 696–706.
695 doi:10.1093/aje/145.8.696
- 696 Lipsitz, L.A., Goldberger, A.L., 1992. Loss of ‘Complexity’ and Aging: Potential
697 Applications of Fractals and Chaos Theory to Senescence. *JAMA J. Am. Med. Assoc.*
698 267, 1806–1809. doi:10.1001/jama.1992.03480130122036
- 699 Loeffler, M., Engel, C., Ahnert, P., Alfermann, D., Arelin, K., Baber, R., Beutner, F., Binder,
700 H., Brähler, E., Burkhardt, R., Ceglarek, U., Enzenbach, C., Fuchs, M., Glaesmer, H.,
701 Girlich, F., Hagendorff, A., Häntzsch, M., Hegerl, U., Henger, S., Hensch, T., Hinz, A.,
702 Holzendorf, V., Husser, D., Kersting, A., Kiel, A., Kirsten, T., Kratzsch, J., Krohn, K.,
703 Luck, T., Melzer, S., Netto, J., Nüchter, M., Raschpichler, M., Rauscher, F.G., Riedel-
704 Heller, S.G., Sander, C., Scholz, M., Schönknecht, P., Schroeter, M.L., Simon, J.-C.,
705 Speer, R., Stäker, J., Stein, R., Stöbel-Richter, Y., Stumvoll, M., Tarnok, A., Teren, A.,
706 Teupser, D., Then, F.S., Tönjes, A., Treudler, R., Villringer, A., Weissgerber, A.,
707 Wiedemann, P., Zachariae, S., Wirkner, K., Thiery, J., 2015. The LIFE-Adult-Study:
708 objectives and design of a population-based cohort study with 10,000 deeply phenotyped
709 adults in Germany. *BMC Public Health* 15, 691. doi:10.1186/s12889-015-1983-z
- 710 Lohmann, G., Margulies, D.S., Horstmann, A., Pleger, B., Lepsien, J., Goldhahn, D.,
711 Schloegl, H., Stumvoll, M., Villringer, A., Turner, R., 2010. Eigenvector centrality
712 mapping for analyzing connectivity patterns in fMRI data of the human brain. *PLoS One*
713 5, e10232. doi:10.1371/journal.pone.0010232
- 714 Mahinrad, S., Jukema, J.W., Van Heemst, D., MacFarlane, P.W., Clark, E.N., De Craen,
715 A.J.M., Sabayan, B., 2016. 10-Second heart rate variability and cognitive function in old
716 age. *Neurology* 86, 1120–1127. doi:10.1212/WNL.0000000000002499
- 717 Maier, S.U., Hare, T.A., 2017. Higher Heart-Rate Variability Is Associated with
718 Ventromedial Prefrontal Cortex Activity and Increased Resistance to Temptation in

- 719 Dietary Self-Control Challenges. *J. Neurosci.* 37, 446–455.
720 doi:10.1523/JNEUROSCI.2815-16.2017
- 721 Makovac, E., Garfinkel, S., Bassi, A., Basile, B., Macaluso, E., Cercignani, M., Calcagnini,
722 G., Mattei, E., Mancini, M., Agalliu, D., Cortelli, P., Caltagirone, C., Critchley, H.,
723 Bozzali, M., 2017. Fear processing is differentially affected by lateralized stimulation of
724 carotid baroreceptors. *Cortex.* 99, 200–212. doi:10.1016/j.cortex.2017.07.002
- 725 Marques, J.P., Kober, T., Krueger, G., van der Zwaag, W., Van de Moortele, P.F., Gruetter,
726 R., 2010. MP2RAGE, a self bias-field corrected sequence for improved segmentation
727 and T1-mapping at high field. *Neuroimage* 49, 1271–1281.
728 doi:10.1016/j.neuroimage.2009.10.002
- 729 Mather, M., Thayer, J.F., 2018. How heart rate variability affects emotion regulation brain
730 networks. *Curr. Opin. Behav. Sci.* 19, 98–104. doi:10.1016/j.cobeha.2017.12.017
- 731 McEwen, B.S., 2003. Interacting mediators of allostasis and allostatic load: Towards an
732 understanding of resilience in aging. *Metabolism.* 52, 10–16. doi:10.1016/S0026-
733 0495(03)00295-6
- 734 Molfino, A., Fiorentini, A., Tubani, L., Martuscelli, M., Fanelli, F.R., Laviano, A., 2009.
735 Body mass index is related to autonomic nervous system activity as measured by heart
736 rate variability. *Eur. J. Clin. Nutr.* 63, 1263–1265. doi:10.1038/ejcn.2009.35
- 737 Munoz, M.L., Van Roon, A., Riese, H., Thio, C., Oostenbroek, E., Westrik, I., De Geus,
738 E.J.C., Gansevoort, R., Lefrandt, J., Nolte, I.M., Snieder, H., 2015. Validity of (Ultra-
739)Short recordings for heart rate variability measurements. *PLoS One* 10, 1–15.
740 doi:10.1371/journal.pone.0138921
- 741 Nussinovitch, U., Elishkevitz, K.P., Kaminer, K., Nussinovitch, M., Segev, S., Volovitz, B.,
742 Nussinovitch, N., 2011a. The efficiency of 10-second resting heart rate for the evaluation
743 of short-term heart rate variability indices. *PACE - Pacing Clin. Electrophysiol.* 34,

- 744 1498–1502. doi:10.1111/j.1540-8159.2011.03178.x
- 745 Nussinovitch, U., Elishkevitz, K.P., Katz, K., Nussinovitch, M., Segev, S., Volovitz, B.,
746 Nussinovitch, N., 2011b. Reliability of ultra-short ECG indices for heart rate variability.
747 *Ann. Noninvasive Electrocardiol.* 16, 117–122. doi:10.1111/j.1542-474X.2011.00417.x
- 748 Porges, S.W., 2007. The polyvagal perspective. *Biol. Psychol.* 74, 116–143.
749 doi:10.1016/j.biopsycho.2006.06.009
- 750 Porges, S.W., 2001. The polyvagal theory: Phylogenetic substrates of a social nervous system.
751 *Int. J. Psychophysiol.* 42, 123–146. doi:10.1016/S0167-8760(01)00162-3
- 752 Porges, S.W., 1995. Orienting in a Defensive World. *Psychophysiology.*
- 753 Posner, J., Cha, J., Wang, Z., Talati, A., Warner, V., Gerber, A., Peterson, B.S., Weissman,
754 M., 2016. Increased Default Mode Network Connectivity in Individuals at High Familial
755 Risk for Depression. *Neuropsychopharmacology* 41, 1759–1767.
756 doi:10.1038/npp.2015.342
- 757 Power, J.D., Barnes, K.A., Snyder, A.Z., Schlaggar, B.L., Petersen, S.E., 2012. Spurious but
758 systematic correlations in functional connectivity MRI networks arise from subject
759 motion. *Neuroimage* 59, 2142–2154. doi:10.1016/j.neuroimage.2011.10.018
- 760 Raichle, M.E., MacLeod, A.M., Snyder, A.Z., Powers, W.J., Gusnard, D.A., Shulman, G.L.,
761 2001. A default mode of brain function. *Proc. Natl. Acad. Sci.* 98, 676–682.
762 doi:10.1073/pnas.98.2.676
- 763 Reitan, R.M., 1955. Certain differential effects of left and right cerebral lesions in human
764 adults. *J Comp Physiol Psychol* 48, 474–477.
- 765 Reitan, R.M., Wolfson, D., 1995. Category Test and Trail Making Test as Measures of
766 Frontal Lobe Functions. *Clin. Neuropsychol.* 9, 50–56.
767 doi:10.1080/13854049508402057
- 768 Rokem, A., Trumpis, M., Perez, F., 2009. Nitime: time-series analysis for neuroimaging data.

- 769 Proc. 8th Python Sci. Conf. (SciPy 2009) 1–8.
- 770 Sacchetti, B., Baldi, E., Lorenzini, C.A., Bucherelli, C., 2002. Cerebellar role in fear-
771 conditioning consolidation. *Proc. Natl. Acad. Sci.* 99, 8406–8411.
772 doi:10.1073/pnas.112660399
- 773 Sakaki, M., Yoo, H.J., Nga, L., Lee, T.-H., Thayer, J.F., Mather, M., 2016. Heart rate
774 variability is associated with amygdala functional connectivity with MPFC across
775 younger and older adults. *Neuroimage* 139, 44–52.
776 doi:10.1016/j.neuroimage.2016.05.076
- 777 Sin, N.L., Sloan, R.P., McKinley, P.S., Almeida, D.M., 2016. Linking Daily Stress Processes
778 and Laboratory-Based Heart Rate Variability in a National Sample of Midlife and Older
779 Adults. *Psychosom. Med.* 78, 573–582. doi:10.1097/PSY.0000000000000306
- 780 Singh, J.P., Larson, M.G., Tsuji, H., Evans, J.C., O'Donnell, C.J., Levy, D., 1998. Reduced
781 heart rate variability and new-onset hypertension: Insights into pathogenesis of
782 hypertension: The Framingham Heart Study. *Hypertension* 32, 293–297.
783 doi:10.1161/01.HYP.32.2.293
- 784 Smith, R., Thayer, J.F., Khalsa, S.S., Lane, R.D., 2017. The hierarchical basis of
785 neurovisceral integration. *Neurosci. Biobehav. Rev.* 75, 274–296.
786 doi:10.1016/j.neubiorev.2017.02.003
- 787 Streitbürger, D.P., Pampel, A., Krueger, G., Lepsien, J., Schroeter, M.L., Mueller, K., Möller,
788 H.E., 2014. Impact of image acquisition on voxel-based-morphometry investigations of
789 age-related structural brain changes. *Neuroimage* 87, 170–182.
790 doi:10.1016/j.neuroimage.2013.10.051
- 791 Swank, A.M., 1996. Physical Dimensions of Aging. *Med. Sci. Sport. Exerc.* 28, 398,399.
792 doi:10.1097/00005768-199603000-00018
- 793 Tarvainen, M.P., Niskanen, J.-P., Lipponen, J.A., Ranta-Aho, P.O., Karjalainen, P.A., 2014.

- 794 Kubios HRV--heart rate variability analysis software. *Comput. Methods Programs*
795 *Biomed.* 113, 210–220. doi:10.1016/j.cmpb.2013.07.024
- 796 Tataranni, P.A., Gautier, J.F., Chen, K., Uecker, A., Bandy, D., Salbe, A.D., Pratley, R.E.,
797 Lawson, M., Reiman, E.M., Ravussin, E., 1999. Neuroanatomical correlates of hunger
798 and satiation in humans using positron emission tomography. *Proc. Natl. Acad. Sci. U. S.*
799 *A.* 96, 4569–74. doi:http://dx.doi.org/10.1073/pnas.96.8.4569
- 800 Taubert, M., Lohmann, G., Margulies, D.S., Villringer, A., Ragert, P., 2011. Long-term
801 effects of motor training on resting-state networks and underlying brain structure.
802 *Neuroimage* 57, 1492–1498. doi:10.1016/j.neuroimage.2011.05.078
- 803 Thayer, J.F., Åhs, F., Fredrikson, M., Sollers, J.J., Wager, T.D., 2012. A meta-analysis of
804 heart rate variability and neuroimaging studies: Implications for heart rate variability as a
805 marker of stress and health. *Neurosci. Biobehav. Rev.* 36, 747–756.
806 doi:10.1016/j.neubiorev.2011.11.009
- 807 Thayer, J.F., Lane, R.D., 2007. The role of vagal function in the risk for cardiovascular
808 disease and mortality. *Biol. Psychol.* 74, 224–242. doi:10.1016/j.biopsycho.2005.11.013
- 809 Thayer, J.F., Lane, R.D., 2000. A model of neurovisceral integration in emotion regulation
810 and dysregulation. *J. Affect. Disord.* 61, 201–216. doi:10.1016/S0165-0327(00)00338-4
- 811 Thayer, J.F., Ruiz-Padial, E., 2006. Neurovisceral integration, emotions and health: An
812 update. *Int. Congr. Ser.* 1287, 122–127. doi:10.1016/j.ics.2005.12.018
- 813 Thayer, J.F., Sollers, J.J., Friedman, B.H., Koenig, J., 2015. Gender differences in the
814 relationship between resting heart rate variability and 24-hour blood pressure variability.
815 *Blood Press.* 7051, 1–5. doi:10.3109/08037051.2016.1090721
- 816 Thayer, J.F., Yamamoto, S.S., Brosschot, J.F., 2010. The relationship of autonomic
817 imbalance, heart rate variability and cardiovascular disease risk factors. *Int. J. Cardiol.*
818 141, 122–131. doi:10.1016/j.ijcard.2009.09.543

- 819 Uddin, L.Q., Kelly, A.M.C., Biswal, B.B., Castellanos, F.X., Milham, M.P., 2009. Functional
820 Connectivity of Default Mode Network Components: Correlation, Anticorrelation, and
821 Causality. *Hum. Brain Mapp.* 30, 625–637. doi:10.1002/hbm.20531
- 822 Umetani, K., Singer, D.H., McCraty, R., Atkinson, M., 1998. Twenty-four hour time domain
823 heart rate variability and heart rate: Relations to age and gender over nine decades. *J.*
824 *Am. Coll. Cardiol.* 31, 593–601. doi:10.1016/S0735-1097(97)00554-8
- 825 Voss, A., Schroeder, R., Heitmann, A., Peters, A., Perz, S., 2015. Short-term heart rate
826 variability - Influence of gender and age in healthy subjects. *PLoS One* 10, e0118308.
827 doi:10.1371/journal.pone.0118308
- 828 Wei, L., Chen, H., Wu, G.R., 2018. Heart rate variability associated with grey matter volumes
829 in striatal and limbic structures of the central autonomic network. *Brain Res.* 1681, 14–
830 20. doi:10.1016/j.brainres.2017.12.024
- 831 Williams, D.P., Cash, C., Rankin, C., Bernardi, A., Koenig, J., Thayer, J.F., 2015. Resting
832 heart rate variability predicts self-reported difficulties in emotion regulation: A focus on
833 different facets of emotion regulation. *Front. Psychol.* 6, 1–8.
834 doi:10.3389/fpsyg.2015.00261
- 835 Wink, A.M., de Munck, J.C., van der Werf, Y.D., van den Heuvel, O.A., Barkhof, F., 2012.
836 Fast Eigenvector Centrality Mapping of Voxel-Wise Connectivity in Functional
837 Magnetic Resonance Imaging: Implementation, Validation, and Interpretation. *Brain*
838 *Connect.* 2, 265–274. doi:10.1089/brain.2012.0087
- 839 Winkelmann, T., Thayer, J.F., Pohlack, S., Nees, F., Grimm, O., Flor, H., 2017. Structural
840 brain correlates of heart rate variability in a healthy young adult population. *Brain Struct.*
841 *Funct.* 222, 1061–1068. doi:10.1007/s00429-016-1185-1
- 842 Wong, S.W., Massé, N., Kimmerly, D.S., Menon, R.S., Shoemaker, J.K., 2007. Ventral
843 medial prefrontal cortex and cardiovagal control in conscious humans. *Neuroimage* 35,

844 698–708. doi:10.1016/j.neuroimage.2006.12.027

845 Yoo, H.J., Thayer, J.F., Greening, S., Lee, T.-H., Ponzio, A., Min, J., Sakaki, M., Nga, L.,
846 Mather, M., Koenig, J., 2017. Brain structural concomitants of resting state heart rate
847 variability in the young and old: evidence from two independent samples. *Brain Struct.*
848 *Funct.* doi:10.1007/s00429-017-1519-7

849 Yu, C., Zhou, Y., Liu, Y., Jiang, T., Dong, H., Zhang, Y., Walter, M., 2011. Functional
850 segregation of the human cingulate cortex is confirmed by functional connectivity based
851 neuroanatomical parcellation. *Neuroimage* 54, 2571–2581.
852 doi:10.1016/j.neuroimage.2010.11.018

853 Zeki Al Hazzouri, A., Haan, M.N., Deng, Y., Neuhaus, J., Yaffe, K., 2014. Reduced heart rate
854 variability is associated with worse cognitive performance in elderly Mexican
855 Americans. *Hypertension* 63, 181–187. doi:10.1161/HYPERTENSIONAHA.113.01888

856 Zulfiqar, U., Jurivich, D.A., Gao, W., Singer, D.H., 2010. Relation of High Heart Rate
857 Variability to Healthy Longevity. *Am. J. Cardiol.* 105, 1181–1185.
858 doi:10.1016/j.amjcard.2009.12.022

859

860 **Supplementary Table 1.** Association (Spearman's rho) between heart rate variability (HRV)
861 and other parameters per age group.

	Young	Middle	Old
Age	-0.10	-0.21*	-0.01
mean FD (mm)	-0.13	-0.11	0.09
BMI (kg/m ²)	0.13	-0.20*	-0.14
WHR	-0.04	-0.17	-0.08
SBP (mmHg)	0.01	-0.17	-0.01
DBP (mmHg)	-0.06	-0.23*	-0.01
TMT A (s)	0.01	-0.12	-0.04
TMT B (s)	-0.06	-0.12	0.02

862 * $p < 0.05$; ** $p < 0.01$; *** $p < 0.001$, 2-tailed.

863 *Note.* FD = framewise displacement; BMI = body mass index; WHR = waist to hip ratio; SBP

864 = systolic blood pressure; DBP = diastolic blood pressure, TMT = trail making test.